



Magnetically coupled pancake vortex molecules in $\text{HgBa}_2\text{Ca}_{n-1}\text{Cu}_n\text{O}_y$ ($n \geq 6$)

A. Crisan,^{1,2,3,*} A. Iyo,³ Y. Tanaka,³ H. Matsuhata,³ D. D. Shivagan,³ P. M. Shirage,³ K. Tokiwa,⁴ T. Watanabe,⁴ T. W. Button,¹ and J. S. Abell¹

¹*Department of Metallurgy and Materials, University of Birmingham, Birmingham B15 2TT, United Kingdom*

²*National Institute of Materials Physics Bucharest, Bucharest 077125, Romania*

³*National Institute of Advanced Industrial Science and Technology, Tsukuba 305-8568, Japan*

⁴*Department of Applied Electronics, Science University of Tokyo, Noda 278-851, Japan*

(Received 18 July 2007; published 21 April 2008)

As recently shown, $\text{HgBa}_2\text{Ca}_{n-1}\text{Cu}_n\text{O}_y$ ($n \geq 6$) cuprate superconductors have a critical temperature of about 100 K independent of n . This remarkable property can be explained by the very imbalanced distribution of carriers among the inequivalent CuO_2 planes in the unit cell. We discovered that these materials also have a common vortex melting line that resembles the theoretical melting lines of magnetically coupled pancake vortices. We suggest that there are two types of pancake pairs situated in the superconducting CuO_2 outer planes: those separated by the thin charge reservoir layer are strongly (Josephson) coupled, while those separated by the thick block of $(n-2)$ CuO_2 nonsuperconducting inner planes are weakly (magnetically) coupled, forming magnetically coupled pancake vortex molecules.

DOI: 10.1103/PhysRevB.77.144518

PACS number(s): 74.25.Qt, 74.25.Ha, 74.72.Jt

I. INTRODUCTION

High- T_c superconductors (HTSs) have a very rich vortex phase diagram.¹ A quite recent addition was the discovery of one-dimensional chains of pancake vortex stacks trapped by the Josephson vortices,² as theoretically predicted.³ In layered HTSs, the case of vanishing short-range Josephson coupling, in which the interaction between pancake vortices is provided by the long-range magnetic coupling was only theoretically discussed up until now.⁴⁻⁶

Multilayered ($n=3-5$) and supermultilayered ($n \geq 6$) $\text{HgBa}_2\text{Ca}_{n-1}\text{Cu}_n\text{O}_y$ [$\text{Hg-12}(n-1)n$] are composed of a charge reservoir layer (CRL) HgBa_2O_x and of the infinite layer (IL) $\text{Ca}_{n-1}\text{Cu}_n\text{O}_{2n}$, where n is the number of CuO_2 planes between two CRLs that supply holes to the above-mentioned CuO_2 planes. They include crystallographically inequivalent CuO_2 planes in a unit cell, outer planes (OPs) with pyramidal (five) oxygen coordination, and inner planes (IPs) with square (four) oxygen coordination, usually with an inhomogeneous charge distribution between OPs and IPs. In Hg-1245 , it was shown that the two optimally doped OPs undergo a superconducting (SC) transition at $T_c=108$ K, whereas the three underdoped IPs have an antiferromagnetic transition below $T_N \approx 60$ K.^{7,8}

Another interesting property is the dependence of T_c on the number of CuO_2 planes, n . In $\text{Hg-12}(n-1)n$, a maximum T_c of about 135 K is obtained for $n=3$, then T_c decreases to 125 K ($n=4$), to 108 K ($n=5$), and to about 100 K ($n=6$). Quite astonishingly, for n between 6 and 9, $\text{Hg-12}(n-1)n$ retains a high and almost constant T_c of about 100 K, as revealed by dc magnetization and ac susceptibility measurements.⁹

Here, we show that for $n \geq 6$, T_c is independent of n , even in high magnetic fields, and that the vortex melting lines are identical. The common vortex melting line of $\text{Hg-12}(n-1)n$ ($n \geq 6$) looks qualitatively similar to those theoretically calculated in the case of magnetically coupled pancake vortices, a fact that can be explained by a vanishing Josephson cou-

pling and a finite long-range magnetic coupling between pancakes situated on the two CuO_2 OPs separated by the $(n-2)$ CuO_2 IPs. Unlike the theoretical models of magnetically coupled pancakes, in $\text{Hg-12}(n-1)n$ ($n \geq 6$) the Josephson coupling between pancakes in two outer planes separated by the thin HgBa_2O_x CRL is strong enough, suggesting the possibility of a new phase of vortex matter, which could be called *magnetically coupled pancake vortex molecules*.

II. EXPERIMENT

Various samples were synthesized from HgO , CuO , Cu_2O , Ca_2CuO_3 , and the precursor $\text{Ba}_2\text{Ca}_2\text{Cu}_3\text{O}_{\sim 7.5}$ or $\text{Ba}_{0.94}\text{Cu}_{1.06}\text{O}_y$. The precursors were prepared from a mixture of Ca_2CuO_3 , CuO , and BaO_2 by heating at 910–940 °C for 12 h in flowing oxygen. Combining source materials, mixtures with nominal compositions $\text{HgBa}_2\text{Ca}_{n-1}\text{Cu}_n\text{O}_{2n+2+\delta}$ ($n=4-14$) were obtained, pressed into pellets, encapsulated in Au, and heated at 1000–1100 °C under a pressure of 3.5 GPa for 2 h.

For the present study, the as synthesized samples were ground, mixed with epoxy resin in a 1:3 weight ratio, and aligned in a magnetic field of 7 T, for 10–12 h, at room temperature. The preparation is described in detail elsewhere.⁹⁻¹¹

The samples were characterized by x-ray diffraction (XRD) (for both powdered and grain-aligned samples), by using an energy dispersive x-ray analyzer attached to a scanning electron microscope (SEM-EDX) to check the cation ratio, and by transmission electron microscopy (TEM). The superconducting properties were studied by four-probe electrical resistivity (for the as-grown samples), by temperature-dependent dc susceptibility (Magnetic Properties Measurement System, Quantum Design), and by multiharmonic ac susceptibility (Physical Properties Measurement System, Quantum Design).

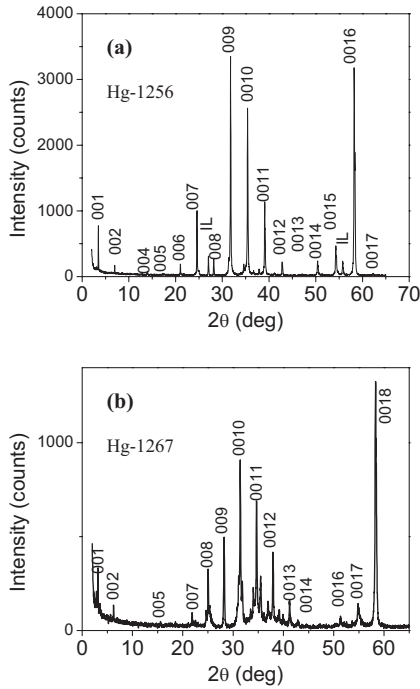


FIG. 1. X-ray diffraction patterns of (a) Hg-1256 and (b) Hg-1267 with the grains aligned in high magnetic fields. Apart from a small amount of the IL phase, only the (00 l) lines of the nominal phase are present.

III. RESULTS AND DISCUSSION

A. Structural characterization

Quite important for our study are the XRD patterns of the grain-aligned samples. For n between 4 and 7, XRD patterns showed only $[N_h(\text{OP})]$ lines of the nominal phase, in some cases with a small amount (few percent) of impurity (n different from the nominal one), as stacking faults, or a very small amount of CaCuO_2 IL. Presented in Fig. 1 are such XRD patterns of (a) Hg-1256 showing (00 l) lines of the nominal phase and a very small amount of IL and (b) Hg-1267 showing (00 l) of the nominal phase, a small amount of Hg-1278 [only (00 l) lines], and a very small amount of an unidentified phase, which is without any superconducting properties, with this phase appearing also in some IL samples.

The samples with the nominal compositions Hg-1278 ($n=8$), Hg-12910 ($n=10$), and Hg-121314 ($n=14$), showed only (00 l) lines of a large number of phases with n between 5 and 16. Such an example is given in Fig. 2 for the sample with the nominal composition Hg-12910 ($n=10$); a more detailed discussion on the XRD patterns of supermultilayered Hg-based cuprates can be found in Ref. 11.

To obtain microscopic information, we performed compositional analysis on the grains by using SEM-EDX and observed the lattice images by using TEM. The resulting average cation ratio, which was measured for many grains, is very close to the nominal ones.¹¹ From transmission electron microscopy, we have seen in fact that for the $n=8, 10,$ and 14 (nominal) samples, the grains consist of stacking sequences, which are randomly distributed along the c axis, of various

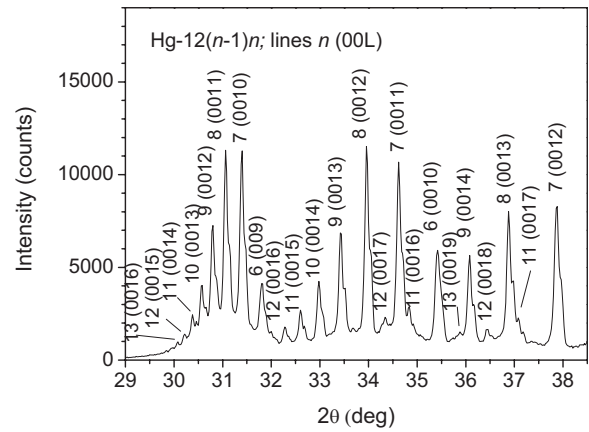


FIG. 2. X-ray diffraction pattern of the Hg-12910 aligned sample showing only (00 l) lines of Hg-12($n-1$) n phases with n between 6 and 14.

$[N_h(\text{IP})]$ layers with n between 5 and 16. Such an image is shown in Fig. 3 for the case of Hg-12910 sample, as projected along the $[001]$ direction. The bright lines correspond to the HgO_y planes in the $\text{HgBa}_2\text{O}_{2+y}$ charge reservoir layer, and the numbers of CuO_2 planes between the CRLs are given in Fig. 3. The TEM images on other grains and on other Hg-12($n-1$) n ($n \geq 8$) look similar, although with other stacking sequences.

B. Independence of critical current density on n for $n \geq 6$

As previously reported,⁹ samples Hg-1256 and Hg-1267, which are almost single phase, have the same critical temperature T_c of about 100 K. In the case of multiphase samples Hg-12($n-1$) n ($n \geq 8$), magnetization^{10,11} and ac susceptibility measurements (present study) showed *only one* large and relatively sharp superconducting transition at about 100 K, indicating that for large n between 6 and 15, Hg-12($n-1$) n phases have a $[N_h(\text{OP})]$ -independent T_c . Otherwise, the superconducting transition would have been step-like. Only in a logarithmic plot very small diamagnetic signals can be seen at about 130 K (very small amount of Hg-

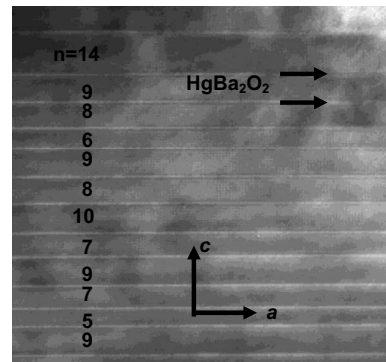


FIG. 3. High resolution transmission electron microscopy of a grain in the Hg-12910 sample. The black arrows indicate the positions of charge reservoir layers (CRL, brighter horizontal lines in the image), while n between 5 and 14 represents the number of CuO_2 planes between two CRLs.

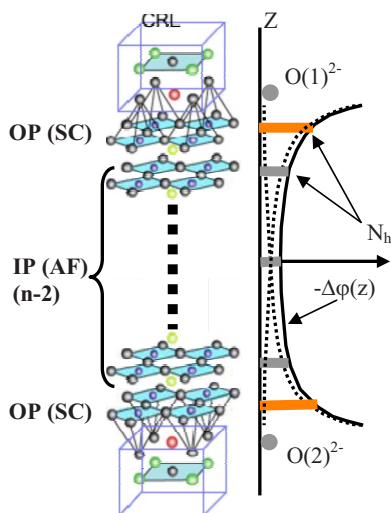


FIG. 4. (Color online) Schematic of the crystal structure of Hg-12($n-1$) n . Between the two HgBa₂O_x CRLs, there are two CuO₂ outer planes sustaining superconductivity, while the ($n-2$) CuO₂ inner planes have a much smaller carrier concentration. The right-hand side shows the very simple model of the z -axis dependence of the electrostatic potential from the two apical oxygen ions (dotted lines) and their sum (full line). For large enough n , the carrier concentration (horizontal thick lines) in the outer planes $N_h(\text{OP})$ comes only from the nearest oxygen ion, the contribution from the ion farther away becoming negligible.

1223, as stacking faults) and about 120 K (Hg-1245, again as stacking faults),¹¹ but no steplike features can be seen below 100 K. One can argue that for multiphase samples, one phase with a lower n might “take over,” but this would not explain the same T_c for Hg-1256 and Hg-1267, which are almost single phase and have almost the same diamagnetic signal. In addition, from the diamagnetic response, we have found that volume fractions (calculated without taking into account demagnetization effects) of samples $n=6, 8, 10$, and 14 are, respectively, 86%, 82%, 83%, and 69%, which are sufficiently large to assume that our multiphase grains can be regarded as bulk superconductors, and, indeed, Hg-12($n-1$) n ($n \geq 6$) phases have a n -independent T_c .

This rather remarkable property can be explained by taking into account the crystal structure of supermultilayered cuprates and the inhomogeneous carrier distribution. Similar to Hg-1245, wherein the optimum doped outer planes are superconducting, while the three, heavily underdoped, inner planes can become antiferromagnetic, in Hg-12($n-1$) n only the two CuO₂ outer planes near the charge reservoir layer contribute to superconductivity, while the ($n-2$) inner planes have a very small carrier concentration and are in an antiferromagnetic state, as shown on the left-hand side of Fig. 4. A constant and high T_c for $n \geq 6$ means that the outer planes can have enough carriers [$N_h(\text{OP})$] for superconductivity, even for large n , while the carrier concentration in inner planes [$N_h(\text{IP})$] is very small and does not contribute to the superconducting transition. At the same time, in order to have a T_c independent of n it is necessary for [$N_h(\text{OP})$] to be independent of n for large n , a fact that can be qualitatively explained by a model, which was introduced for multilayered

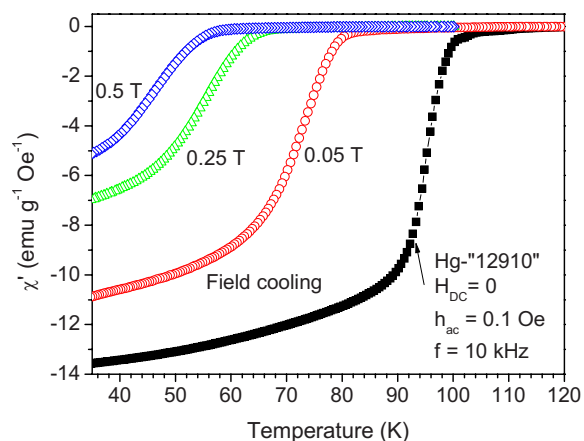


FIG. 5. (Color online) Temperature dependence of the in-phase ac susceptibility of the Hg-12910 sample in zero field and in dc fields of 0.05, 0.25, and 0.5 T.

cuprates.¹² The model shows that the carrier distribution (N_h) among the CuO₂ planes correlates well with the sum of the electrostatic potentials ($-\Delta\phi(Z) \sim 1/Z$) from the two apical oxygen ions, as can be seen in the right-hand side of Fig. 4, wherein the dotted lines represent the electrostatic potentials, the full line is the sum of $-\Delta\phi(Z)$ from the two apical oxygen ions, and the horizontal thick lines represent the carrier concentration of various CuO₂ planes. In this very simple model, it can be seen that for very large n , the contribution from the farther O²⁻ ion to $N_h(\text{OP})$ becomes negligible compared to the contribution from the near O²⁻ ion, which means that $N_h(\text{OP})$ does not depend on n for large n ; hence, T_c is also independent of n .

C. Superconducting transition in dc magnetic fields

To our surprise, even in quite large dc magnetic fields H_{dc} , “Hg-12910” still has only one SC transition. This is rather unexpected since it is common knowledge that the degree to which a dc field would decrease T_c quite strongly depends on the coupling between pancake vortices, hence, on the number of CuO₂ layers. So, one would have expected that an applied dc field would have led to a steplike transition in our multiphase samples. Figure 5 shows the superconducting transition of our Hg-12910 multiphase sample in zero field and in dc fields of 0.05, 0.25, and 0.5 T. No steplike features are present. Quite interestingly, unlike most of superconducting cuprates, it seems that in our Hg-12($n-1$) n ($n \geq 6$) materials, even a moderate dc field strongly decreases the critical temperature. For example, in only 0.05 T, T_c is reduced from about 100 to about 80 K, while in 0.5 T, T_c is reduced by more than 40%. As a comparison, in Hg-1234 the same field of 0.5 T decreases T_c by about 8%. Figure 6 shows the ac susceptibility response in $H_{\text{dc}}=0.05$ T of the 12910 sample, and, for comparison, of the two (almost) single-phase samples, Hg-1256 and Hg-1267. Remarkably, it can be seen that Hg-1256 and Hg-1267 samples still have the same T_c , even in a dc field, while 12910 apparently has a slightly lower one. The apparent lower T_c of 12910 can be easily explained by the fact that in a grain of 12910, the number of

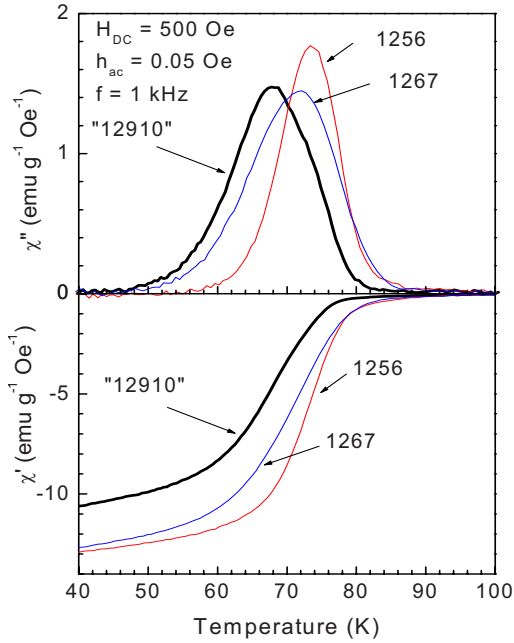


FIG. 6. (Color online) Temperature dependence of (a) in-phase and (b) out-of-phase ac susceptibilities of Hg-1256, Hg-1267, and Hg-12910 in a dc field of 500 Oe.

CuO₂ outer planes that sustain superconducting currents are significantly smaller than those in a grain of Hg-1256 with the same thickness; hence, for the same ac field amplitude, as is the case with our measurements, the same probing current has to be sustained by a smaller number of superconducting outer planes. Consequently, the superconducting outer planes in 12910 sample were probed by a larger sheet current density. This is also the reason for the slightly smaller diamagnetic response of 12910 sample, as compared to those of Hg-1256 and Hg-1267 samples.

D. Vortex melting lines

One of the most important aspects regarding vortex dynamics is the melting line for vortex matter, $B_m(T)$ or $T_m(B)$, which separates the vortex-glass (or solid) (VG) and vortex-liquid (VL) phases.¹³ Recently, we developed a simple and straightforward technique for determining melting lines by using the on set of third-harmonic susceptibility response, χ_3 of bulk superconductors with preferentially oriented crystallites, with very low ac field amplitudes, which proved to be very suitable, especially for these polycrystalline samples grown by high-pressure synthesis.^{14–16} Previously, the on set of the third-harmonic susceptibility was used for the determination of irreversibility lines or flux penetration into a Campbell regime,¹⁷ or for the determination of the Bose-glass transitions in heavy-ion irradiated single crystals.¹⁸

The principle of the method comes from the very basic properties of vortex matter. In the VG state below $T_m(B)$, the electric field response to a current density J is strongly nonlinear, of the form $E(J) \sim \exp[-(J_T/J)^\mu]$, where J_T is a characteristic current density and $\mu \leq 1$, while for $T > T_m(B)$ (in the VL state), one expects an Ohmic behavior $E(J) \sim J$ for sufficiently low current levels. At the same time, the out-of-

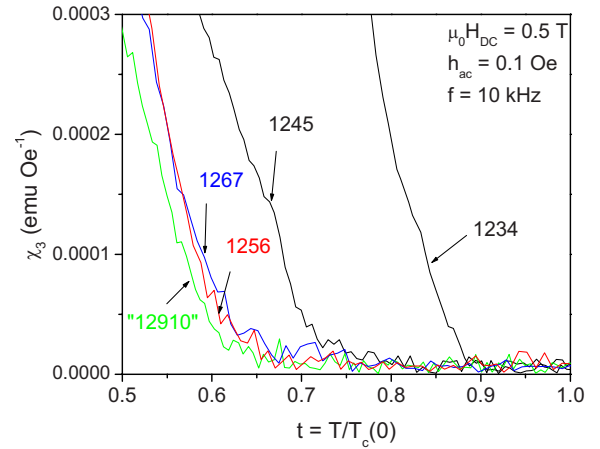


FIG. 7. (Color online) Third-harmonic susceptibilities of Hg-1234, Hg-1245, Hg-1256, Hg-1267, and Hg-12910 as a function of reduced temperature.

phase susceptibility response of a superconductor χ'' is a measure of the total dissipation, linear and nonlinear, while χ_3 is a measure of the nonlinear dissipation only.¹⁹ The measurements were performed by using a Quantum Design PPMS, in fields of up to 7 T, with ac field amplitudes of 0.1 Oe (ensuring in this way a low probing current). Figure 7 presents such measurements of χ_3 as a function of reduced temperature, $t = T/T_c(0)$, for multilayered and supermultilayered Hg cuprates (1234, 1245, 1256, 1267, and 12910), in $H_{dc} = 0.5$ T. It can be clearly seen that Hg-12($n-1$) n ($n \geq 6$) phases have practically the same on set of χ_3 , which represents the reduced melting temperature $t_m(H_{dc})$. Moreover, it can be seen that the amplitudes of $\chi_3(t)$ of the three samples are practically the same, which is another experimental proof that is ruling out the scenario of one phase with lower n “taking over” in respect with the superconducting properties.

Several such measurements, in various H_{dc} , resulted in the experimental melting lines, which are shown in Fig. 8. Again, it can be seen that Hg-1256, Hg-1267, Hg-12910, and Hg-121314 *have practically the same melting line*. Analysis of the melting transition in the framework of an anisotropic three-dimensional (3D) Ginzburg–Landau rescaling approach²⁰ gives the temperature-dependent melting field,

$$B_m(T) = \frac{C^2 c_L^4 \phi_0^5}{(k_B T)^2 \lambda_{ab}^4 \gamma (\cos^2 \alpha + \gamma^2 \sin^2 \alpha)^{1/2}},$$

where C is a constant ($C \approx 1/4\pi^2$), c_L is the empirical Lindemann parameter (about 0.15), ϕ_0 is the magnetic flux quanta, λ_{ab} is the penetration depth along the superconducting (a, b) plane, γ is the anisotropy factor, and α is the angle between the magnetic field lines and the (a, b) plane. For our preferentially oriented samples and with our experimental setup, $\alpha = 90^\circ$.

The full lines in Fig. 8 represent one-parameter fits (anisotropy factor γ being the free parameter) of the melting lines of Hg-1234 and Hg-1245, taking the temperature dependence of λ_{ab} from the “two-fluid” model, $\lambda_{ab}(T) = \lambda_{ab}(0)[1 - (T/T_c)^4]^{-1/2}$, this model giving better results in

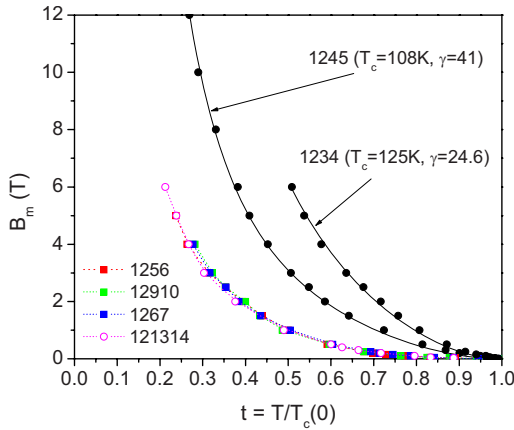


FIG. 8. (Color online) Experimentally determined (symbols) vortex melting lines of Hg-1234, Hg-1245, Hg-1256, Hg-1267, Hg-12910, and Hg-121314. The full lines in the case of Hg-1234 and Hg-1245 represent a one-parameter fit with the model discussed in the text.

terms of quality of the fits as compared to the critical behavior of the 3D XY model, or with the mean-field model. The common melting line of Hg-1256, Hg-1267, Hg-12910, and Hg-121314 could not be successfully fitted to the above-mentioned model, but it resembles very much the theoretical (numerically calculated) melting lines of magnetically coupled pancake vortices, i.e., in the absence of the Josephson coupling.^{4,6}

E. Magnetically coupled pancake vortex molecules

In our opinion, the explanation for these remarkable properties of vortex matter in supermultilayered Hg-based cuprates resides in the interplay between the Josephson coupling Λ_J and the magnetic coupling Λ_m . At short distances, the Josephson coupling is much stronger than the magnetic coupling, while, since Josephson coupling is a short-range interaction, at large distances the magnetic coupling (a long-range interaction) takes over as the dominant pancake-pancake interaction. As can be seen from Fig. 8, Hg-1234 has a very robust melting line that can be very well described by the model described in Sec. III D, with one fitting parameter, anisotropy factor γ , which has a quite small value of about 24.6, which means a quite strong Josephson coupling. Insertion of another CuO_2 inner plane (i.e., leading to Hg-1245 phase) results in a significant shifting of the melting line toward lower temperatures. A weaker melting line means a smaller Josephson coupling, and a larger γ of about 57.4, as resulted from a similar fit.

Now, it is known that the three inner planes in Hg-1245 have a very low carrier concentration, and they undergo an antiferromagnetic transition.⁸ Another addition of an inner plane, leading to the Hg-1256 phase, results in a further (but less significant) shift of the melting line, but from now on, any more additions of inner planes in the unit cell do not affect the melting lines of supermultilayered Hg-based cuprates.

In our opinion, this means that in Hg-1245, there is still a significant Josephson coupling, Λ_J^{IP} , between the pancake

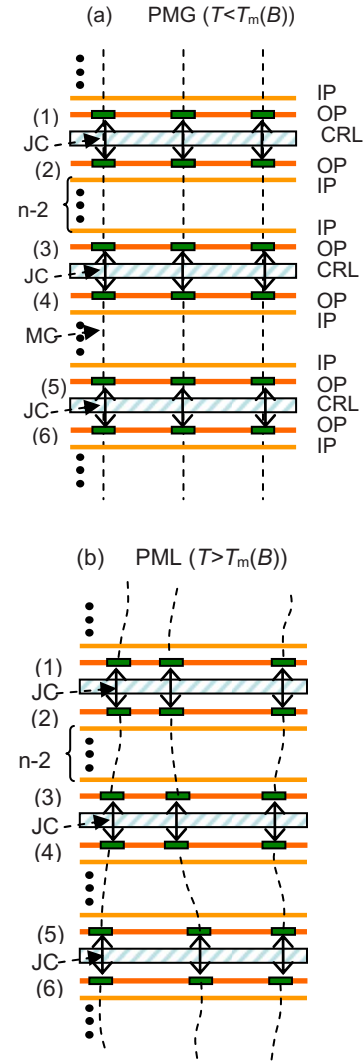


FIG. 9. (Color online) Schematics of the proposed (a) pancake-molecule glass and (b) pancake-molecule liquid. In the case of pancake pairs separated by a thin charge reservoir layer (1-2, 3-4, 5-6), the Josephson coupling is much stronger than the magnetic coupling, while for pancake pairs separated by the thick block of inner planes (2-3, 4-5), the Josephson coupling is much smaller than magnetic coupling. Pancakes (1) and (2), (3) and (4), and (5) and (6) form pancake molecules, which are weakly coupled along the c axis by the magnetic coupling. Upon increasing the temperature, thermal fluctuations overcome the magnetic coupling and the pancake-molecule glass melts into a pancake molecule liquid.

vortices in the two outer planes separated by the three inner planes, while in all other Hg-12($n-1$) n ($n \geq 6$), the short-range Josephson coupling Λ_J^{IP} becomes much smaller than the long-range magnetic coupling, Λ_m^{IP} . Being a long-range pancake-pancake interaction, magnetic coupling Λ_m is not significantly affected by additions of extra inner planes in the unit cell, hence, the common vortex melting line and its resemblance to the theoretical melting lines of magnetically coupled pancakes. However, those theoretical calculations and models^{4,6} consider magnetically coupled pancake vortices that are equally distributed along the c axis (z direction).

That is not our case. As can be seen in Fig. 9, in super-

multilayered Hg-based cuprates, there are two types of pancake pairs: those situated in the outer planes separated by the thick $(n-2)$ inner planes block, for which the Josephson coupling Λ_J^{IP} is much smaller than the magnetic coupling Λ_m^{IP} , and, respectively, those situated in the outer planes separated by the thin charge reservoir layer, for which the Josephson coupling Λ_J^{CRL} is much larger than the magnetic coupling Λ_m^{CRL} . This latter assertion is obvious; otherwise, Hg-1234, for example, would have a very weak melting line. Therefore, the strongly (Josephson) coupled pancake pairs separated by the charge reservoir layer can be regarded as pancake molecules (e.g., pancakes 1 and 2, 3 and 4, and 5 and 6 in Fig. 9) which, in turn, are weakly (magnetically) coupled along the z direction in the solid vortex phase, which can be called the pancake-molecule glass (PMG) (or solid) [Fig. 9(a)]. At higher temperatures, the thermal fluctuations overcome the magnetic coupling, and the PMG melts into a liquid (gas) phase, the pancake molecule liquid [Fig. 9(b)]. Of course, it is expected that at much higher fields, the interaction between pancakes in the same outer plane would be much stronger than the Josephson coupling Λ_J^{CRL} , and the pancake molecules would dissociate into individual pancakes, forming an ideal two-dimensional vortex lattice, as was theoretically predicted^{21,22} and recently proved experimentally²³ for $\text{Bi}_2\text{Sr}_2\text{CaCu}_2\text{O}_{8+\delta}$ in fields larger than 20 T. In our supermultilayered Hg-based cuprates, this dissociation would occur at a much larger field since they have a thinner charge reservoir layer, hence, a stronger Josephson coupling between pancakes separated by CRL.

IV. CONCLUSIONS

We have investigated the family $\text{HgBa}_2\text{Ca}_{n-1}\text{Cu}_n\text{O}_y$ [Hg-12 $(n-1)n$] superconducting cuprates grown by high-pressure synthesis. For $n < 7$, the materials can be grown as single (almost single) phases, while for $n > 7$ the crystals consist of stacking sequences, which are randomly distributed along the c axis, of various Hg-12 $(n-1)n$ layers with n between 5 and 16. We have shown that all of the phases with

$n > 6$ have the same critical temperature, which can be explained by the very unbalanced carrier distribution between the CuO_2 inner planes and outer planes, respectively. Even in applied dc fields, the critical temperature is n independent for $n > 6$ and, unlike the most superconducting cuprates, T_c is strongly reduced by moderate dc fields.

Hg-12 $(n-1)n$ with $n > 6$ have also a common melting line that very well resembles the theoretical melting line of magnetically coupled pancakes. We explain these remarkable properties of vortex matter in the supermultilayered Hg-based cuprates by the interplay between the Josephson coupling and the magnetic coupling between two types of pancake vortex pairs, those separated by the thin charge reservoir layer and those separated by the thick $(n-2)$ CuO_2 inner planes. We suggest that the common vortex melting line separates two phases of vortex matter in high-temperature superconductors: a pancake-molecule solid at lower fields and/or temperatures, which can be either glass or an Abrikosov lattice in the absence of pinning, (which in much higher fields would become a two-dimensional vortex solid), and, respectively, a pancake-molecule liquid (or gas) at higher fields and/or temperatures, which at higher temperatures close to the critical one, at which the London penetration depth diverges, would become a “standard” vortex liquid.

ACKNOWLEDGMENTS

This work was supported by the Japanese Society for the Promotion of Science, by a Grant-in-Aid for Scientific Research on Priority Area “Invention of Anomalous Quantum Materials,” Ministry of Education, Science, Sports and Culture of Japan, by the Romanian Ministry of Education and Research, by the European Commission through the Marie Curie Excellence Grant “NanoTechPinningHTS,” by Japan Science and Technology Agency, and by AIST through germination research initiative “Basic Physics of Multi-band Superconductor” and through the grant for overriding priority research “High- T_c Frontier.”

*Corresponding author; i.a.crisan@bham.ac.uk

¹G. Blatter, M. V. Feigel'man, V. B. Geshkenbein, A. I. Larkin, and V. M. Vinokur, *Rev. Mod. Phys.* **66**, 1125 (1994).

²A. Grigorenko, S. Bending, T. Tamegai, S. Ooi, and M. Henini, *Nature (London)* **414**, 728 (2001).

³A. E. Koshelev, *Phys. Rev. Lett.* **83**, 187 (1999).

⁴M. J. W. Dodgson, A. E. Koshelev, V. B. Geshkenbein, and G. Blatter, *Phys. Rev. Lett.* **84**, 2698 (2000).

⁵R. G. Mints, V. G. Kogan, and J. R. Clem, *Phys. Rev. B* **61**, 1623 (2000).

⁶H. Fangohr, A. E. Koshelev, and M. J. W. Dodgson, *Phys. Rev. B* **67**, 174508 (2003).

⁷K. Tokiwa, H. Okumoto, T. Imamura, S. Mikusu, K. Yuasa, W. Higemoto, K. Nishiyama, A. Iyo, Y. Tanaka, and T. Watanabe, *Int. J. Mod. Phys. B* **17**, 3540 (2003).

⁸H. Kotegawa, Y. Tokunaga, Y. Araki, G.-q. Zheng, Y. Kitaoka,

K. Tokiwa, K. Ito, T. Watanabe, A. Iyo, Y. Tanaka, and H. Ihara, *Phys. Rev. B* **69**, 014501 (2004).

⁹A. Iyo, Y. Tanaka, Y. Kodama, H. Kito, K. Tokiwa, and T. Watanabe, *Physica C* **445-448**, 17 (2006).

¹⁰A. Iyo, Y. Tanaka, H. Kito, H. Matsuhata, K. Tokiwa, and T. Watanabe, *Physica C* **460-462**, 436 (2007).

¹¹A. Iyo, Y. Tanaka, H. Kito, Y. Kodama, P. M. Shirage, D. D. Shivagan, H. Matsuhata, K. Tokiwa, and T. Watanabe, *J. Phys. Soc. Jpn.* **79**, 094711 (2007).

¹²H. Kotegawa, Y. Tokunaga, K. Ishida, G.-q. Zheng, Y. Kitaoka, K. Asayama, H. Kito, A. Iyo, H. Ihara, K. Tanaka, K. Tokiwa, and T. Watanabe, *J. Phys. Chem. Solids* **62**, 171 (2001).

¹³D. S. Fisher, M. P. A. Fisher, and D. A. Huse, *Phys. Rev. B* **43**, 130 (1991).

¹⁴A. Crisan, A. Iyo, and Y. Tanaka, *Appl. Phys. Lett.* **83**, 506 (2003).

- ¹⁵A. Crisan, Y. Tanaka, A. Iyo, L. Cosereanu, K. Tokiwa, and T. Watanabe, *Phys. Rev. B* **74**, 184517 (2006).
- ¹⁶A. Crisan, Y. Tanaka, A. Iyo, D. D. Shivagan, P. M. Shirage, K. Tokiwa, T. Watanabe, L. Cosereanu, T. W. Button, and J. S. Abell, *Phys. Rev. B* **76**, 212508 (2007).
- ¹⁷M. Konczykowski, Y. Wolfus, Y. Yeshurun, and F. Holtzberg, *Physica A* **200**, 305 (1993).
- ¹⁸A. V. Samoilov, M. V. Feigel'man, M. Konczykowski, and F. Holtzberg, *Phys. Rev. Lett.* **76**, 2798 (1996).
- ¹⁹P. Fabbriatore, S. Farinon, G. Gemme, R. Musenich, R. Parodi, and B. Zhang, *Phys. Rev. B* **50**, 3189 (1994).
- ²⁰G. Blatter, V. B. Geshkenbein, and A. I. Larkin, *Phys. Rev. Lett.* **68**, 875 (1992).
- ²¹D. S. Fisher, *Phys. Rev. B* **22**, 1190 (1980).
- ²²L. I. Glazman and A. E. Koshelev, *Phys. Rev. B* **43**, 2835 (1991).
- ²³B. Chen, W. P. Halperin, P. Guptasarma, D. G. Hinks, V. F. Mitrovič, A. P. Reyes, and P. L. Kuhns, *Nat. Phys.* **3**, 239 (2007).